Electronic Supplementary Material (ESI) for Journal of Materials Chemistry A.

Supporting Information

Hierarchical ultrathin-branched CdS nanowire arrays with enhanced photocatalytic performance

Yi Huang,[a] You Xu,[a] Jin Zhang,[a] Xuguang Yin,[a] Yamei Guo[a] and Bin Zhang*[ab]

[a] Department of Chemistry, School of Science, Tianjin University, and Collaborative Innovation Centre of Chemical Science and Engineering (Tianjin), Tianjin 300072, China.

[b] The Key Lab of Systems Bioengineering (Tianjin University), Ministry of Education, Tianjin 300072, China.

E-mail: bzhang@tju.edu.cn

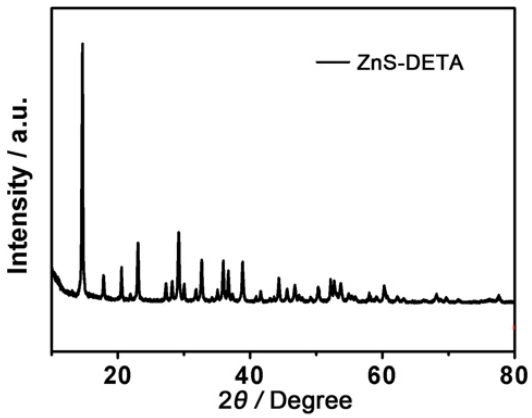

Fig. S1 XRD patterns of ZnS-DETA hybrid nanosheets. The crystal structure of semiconductor-amine is similar with our previous report (Y. F. Yu, J. Zhang, X. Wu, W. Zhao, B. Zhang, *Angew. Chem. Int. Ed.* 2012, 51, 897.), showing that the ZnS-DETA hybird nanosheets have been successfully synthesized. After complete reaction with Cd^{2+}, the inorganic-organic hybrid nanosheets become the inorganic 3DHU-CdS, as displayed in XRD patterns (Figure 2a).

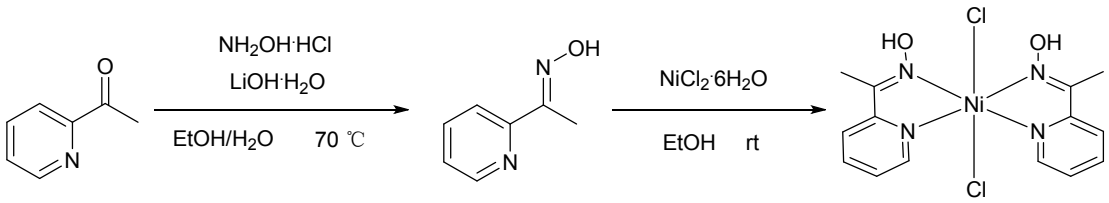

Scheme S1 The synthetic route for Complex **I**.

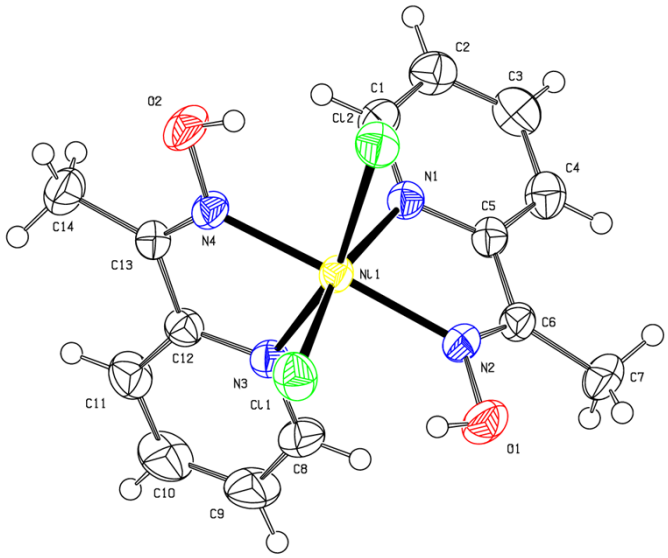

Fig. S2 X-ray crystal structure diagram for Complex **I.**

Table S1 Crystal data and structure refinement for Complex **I**

Bond precision: C-C = 0.0035 A	Wavelength=0.71073	
Cell: a=8.6258(8)	b=10.8561(11)	c=19.8668(17)
alpha=90	beta=114.307(4)	gamma=90
Temperature: 294 K		
	Calculated	Reported
Volume	1695.5(3)	1695.5(3)
Space group	P 21/c	P21/c
Hall group	-P 2ybc	?
Moiety formula	C_{14} H_{16} C_{l2} N_4 Ni O_2	?
Sum formula	C_{14} H_{16} C_{l2} N_4 Ni O_2	C_{14} H_{16} C_{l2} N_4 Ni O_2
Mr	401.90	401.92
Dx,g cm-3	1.574	1.575
Z	4	4
Mu (mm-1)	1.472	1.472
F000	824.0	824.0
F000’	826.75	
h,k,lmax	11, 14, 25	11, 14, 25
Nref	3895	3869
Tmin,Tmax	0.853, 0.929	0.666, 0.930
Tmin’	0.643	
Correction method= MULTI-SCAN		
Data completeness= 0.993	Theta(max)= 27.500	
R(reflections)= 0.0321(3398)	wR2(reflections)= 0.0819(3869)	
S=1.057	Npar=210	

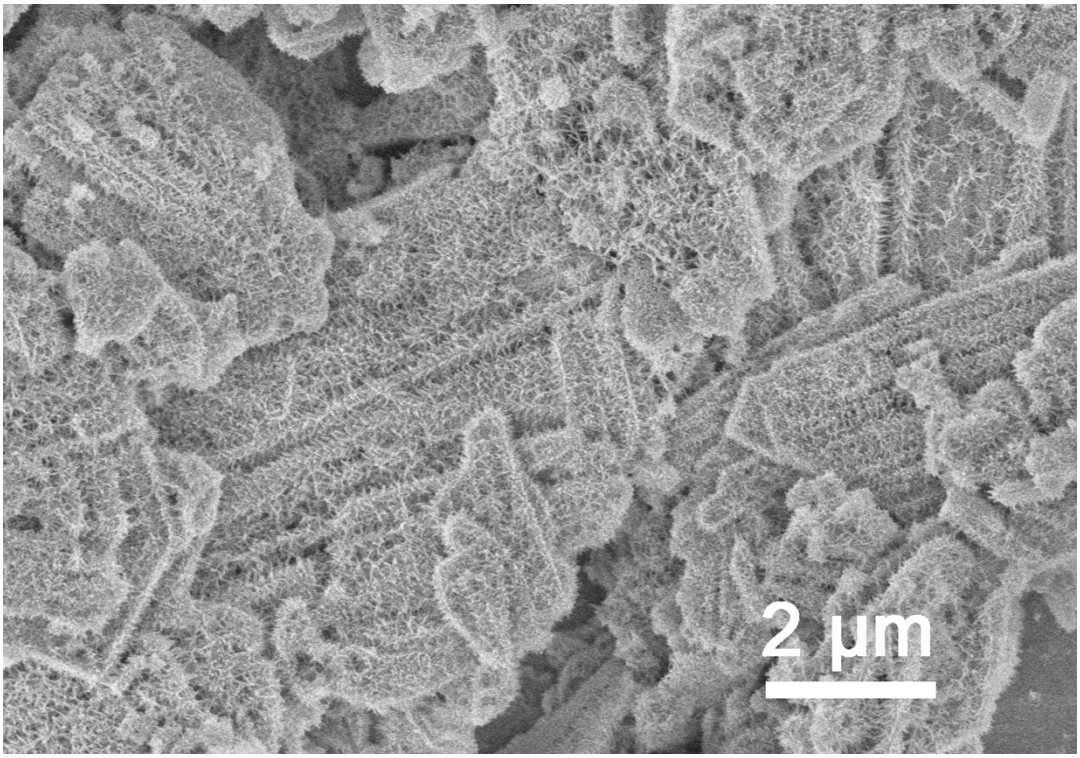

Fig. S3 Low-magnification SEM image of 3DHU-CdS. The solid 2D nanosheets are transformed to branched nanostructure completely, however, the 2D morphology keep unchanged.

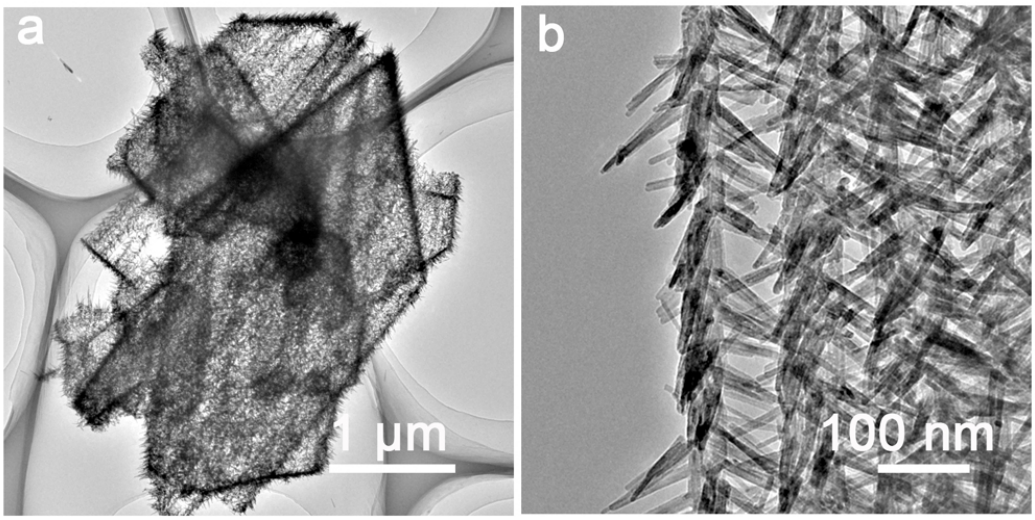

Fig. S4 TEM images of 3DHU-CdS. TEM images further reveal the formation of branched nanowire arrays. The branched nanowires are neatly arrayed so that they can present the form of arrays with the retention of the sheet-like macroscopic morphology. The array structure of branched nanowires become more and more obvious with increasing the reaction temperature (Figure S7c-e).

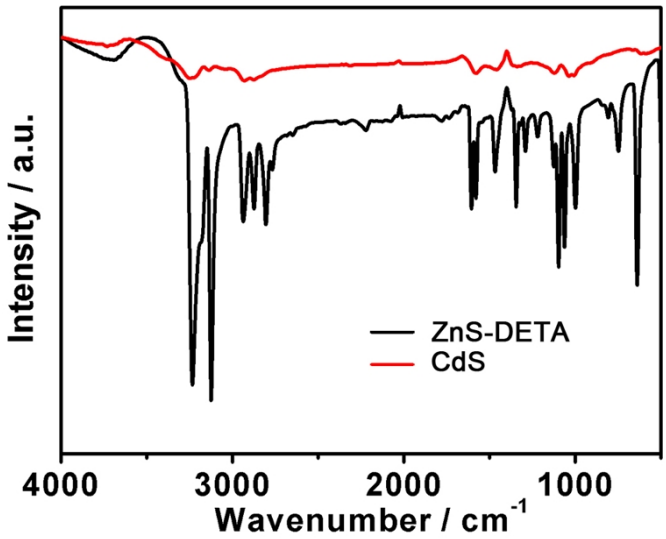

Fig. S5 FTIR spectra of hybrid precursors (blank line) and 3DHU-CdS (red line). The absorption peaks centered at 3300-3400 cm^{-1} and 1532-1680 cm^{-1} can be attributed to the characteristic vibration of N-H stretching and -NH_2 stretching vibration. This indicates that inorganic-organic hybrid nanosheets can be successfully transformed into inorganic materials.

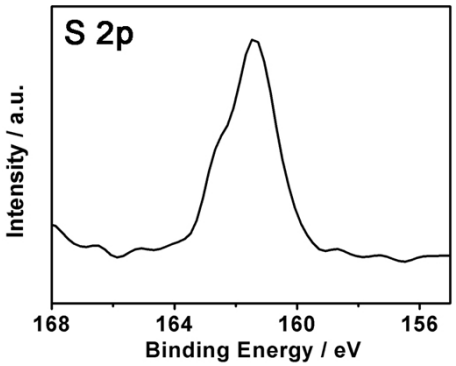

Fig. S6 The high-resolution S 2p XPS spectra of 3DHU-CdS. The low banding energy peaks of S 2p spectra at 161.5 eV is indicative of metal sulfide.

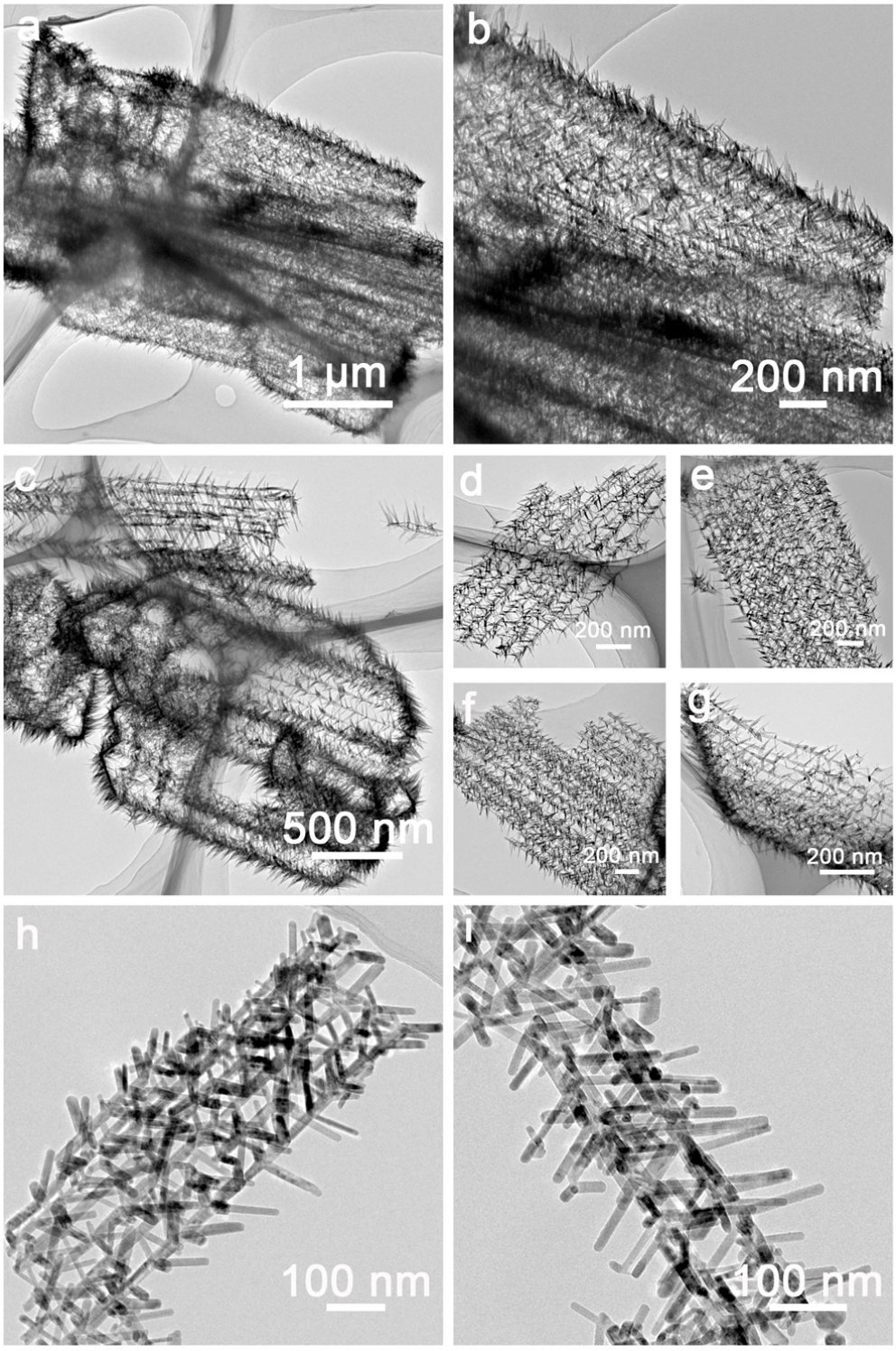

Fig. S7 TEM images of the 3DHU-CdS prepared at different temperatures: (a-b) 80 ℃; (c-g) 160 ℃; (h-i) 220 ℃.

As observed in above TEM images, the hybrid nanosheets can be transformed into 3DHU-CdS at the temperatures ranging from 80 to 220 ℃ and all the products present the form of branched nanowire arrays. The sheet-like morphology can keep unchanged at low temperature (Figure S7a, b). However, with increasing the temperature, the sheet-like morphology are broken to a certain extent, the nanowire arrays are still observed (Figure S7c-i).

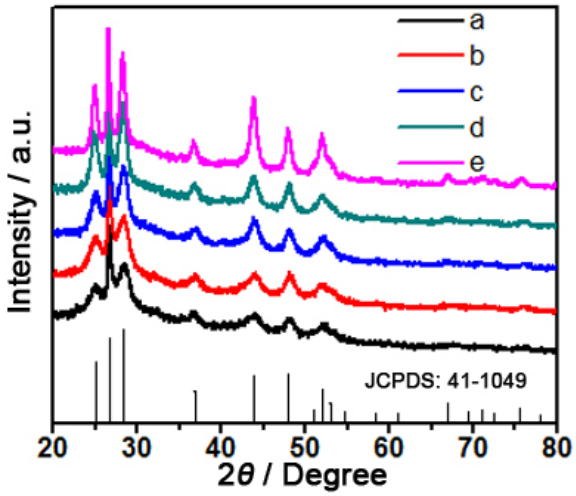

Fig. S8 XRD patterns of the 3DHU-CdS prepared at different temperature: a) 80 ℃; b) 160 ℃; c) 180 ℃; d) 200 ℃; e) 220 ℃. This indicates that all the 3DHU-CdS prepared at different temperature are assigned to hexagonal phase of CdS (JCPDS No. 41-1409).

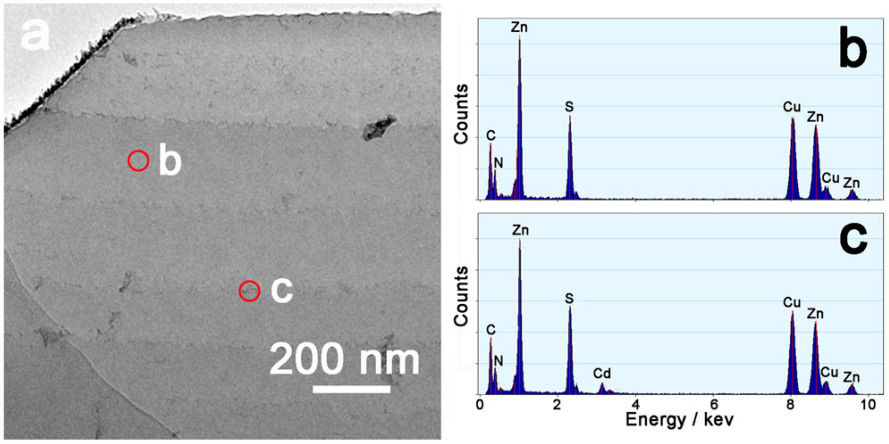

Fig. S9 a) TEM image of the intermediates collected after the reaction of ZnS-DETA with Cd^{2+} ions at 120 ℃ proceeded for 0.5 h. The b and c in (a) indicate the positions where the EDS spectras for (b) and (c) are collected.

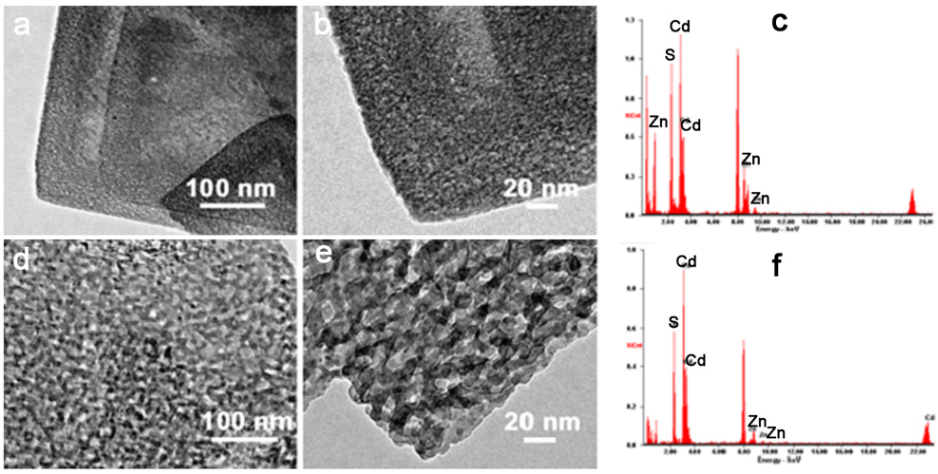

Fig. S10 TEM images (a, b, d, e) and EDS spectras (c, f) of intermediates collected at different stages of cation-exchange reaction in pure water whereas other conditions remain unchanged; (a-c) 0.5 h; (d-f) 3 h. When the cation-exchange reaction proceeds for 0.5h, the sheets become rough with voids (Figure S10 a,b). The associated EDS spectra (Figure S10c) reveals that most of zinc ions in ZnS-DETA have been exchanged with cadmium cation in a very short time, suggesting the rapid kinetic of this cation-exchange reaction. No selectivity on the cation exchange of Cd^{2+} ions with Zn^{2+} ions in hybrid nanosheets is observed. With the continuous increase of the reaction time, the ratio of zinc in $Cd_xZn_{(1-x)}S$-amine is decreasing, and the pores become bigger due to the correlating roles of the strain-driven voids and the dissolution of DETA in aqueous media during cation-exchange reaction (Y. Yu, J. Zhang, X. Wu, W. Zhao, B. Zhang, *Angew. Chem. Int. Ed.* 2012, 51, 897.).

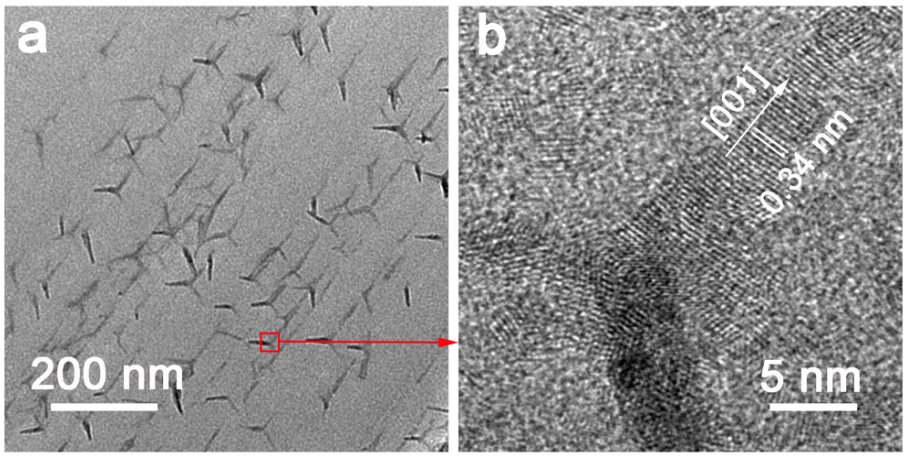

Fig. S11 TEM image and HRTEM image of the intermediates collected after the reaction of ZnS-DETA with Cd^{2+} ions at 120 ℃ proceeded for 2 h.

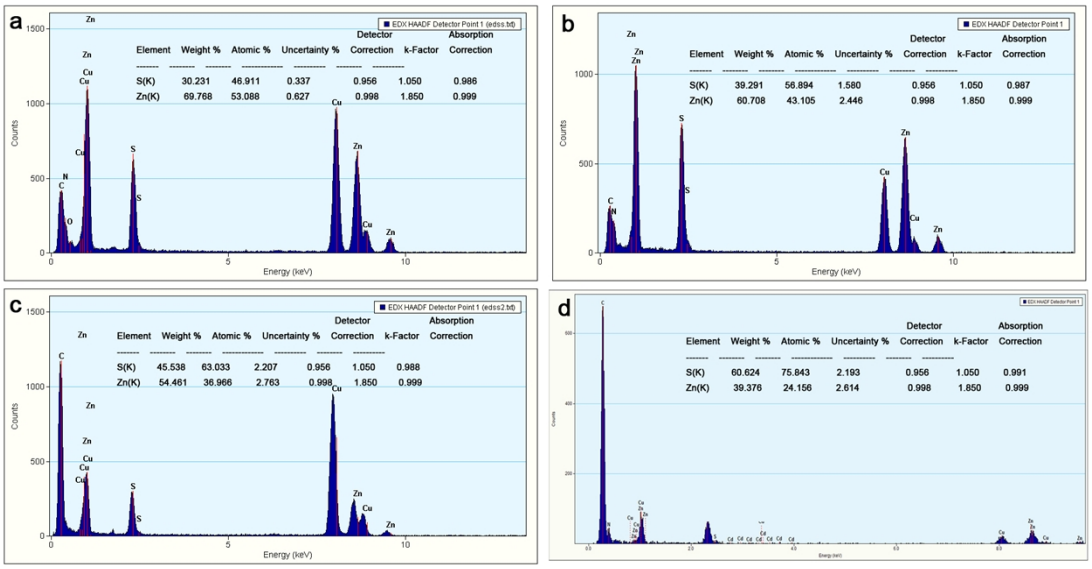

Fig. S12 The point-scan EDS spectras of the stating hybrid nanosheets (a) and the smooth regions on the intermediates: b) 0.5 h; c) 2 h; d) 4 h. The circles in Figure 2d-f indicate the positions where the EDS spectra were obtained. Cu is observed in the spectra and C is not only origin from the nanosheets but also the carbon films because carbon films on copper grids were used as TEM substrates.

Table S2. The summary of the molar ratios of Zn to S of the stating hybrid nanosheets and the smooth regions on the intermediates.

Reaction time (h)	The molar ratio of Zn/S	Error
0	1.029	± 0.022
0.5	0.759	± 0.064
2	0.593	± 0.061
4	0.320	± 0.043

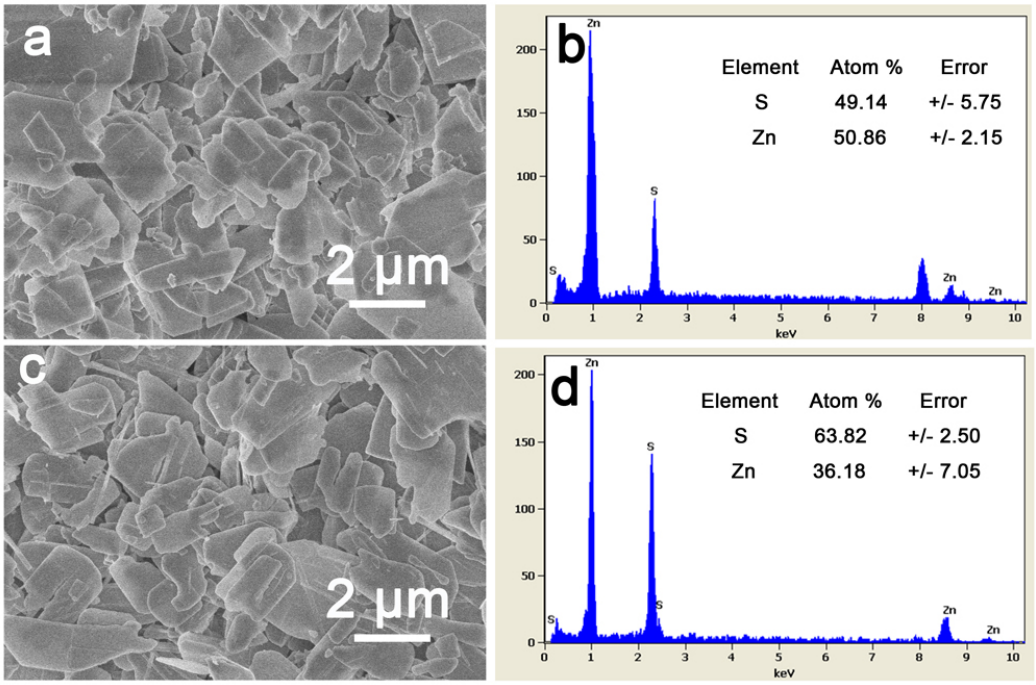

Fig. S13 SEM images (a, c) and EDS spectra (b, d) of the treatment of ZnS-DETA hybrid nanosheets in the mixture solution of DETA and water at 120 ℃ for different time: a, b) 0 h; c, d) 10 h. As shown in this Figure, after the treatment of hybrid nanosheets in the mix solution of DETA and water for 10 h, the morphology of the hybrid nanosheets kept unchanged. However, the relative content of element Zn decreased clearly. In addition, we also collected the supernatants after centrifugation. After adding the excessive Na_2S in supernatant, we could collect the white precipitate which was identified as ZnS by XRD pattern and EDS spectra. These results suggest that Zn^{2+} in the hybrid nanosheets can be extracted by the induced role *via* the coordination of DETA molecules with zinc in the mix solution, as observed in some previous reports (H. Zhang, H. Wang, Y. Xu, S. Zhuo, Y. Yu, B. Zhang, *Angew. Chem. Int. Ed.* 2012, 51, 1459; S. K. Han, C. Gu, M. Gong, S. H. Yu, *J. Am. Chem. Soc.* 2015, 137, 5390.)

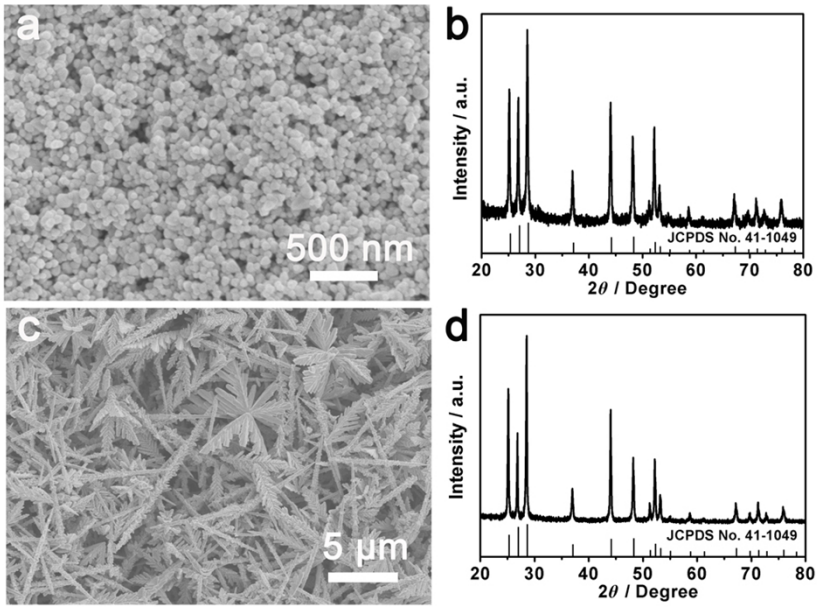

Fig. S14 a-b) SEM image (a) and XRD pattern (b) of CdS NPs. c-d) SEM image (c) and XRD pattern (d) of CdS MDs. The XRD patterns indicate the CdS NPs and CdS MDs all are assigned to hexagonal phase of CdS (JCPDS No. 41-1409).

Table S3. Summary of the band gap values, BET, H_2-production rate and QY of various CdS-based photocatalysts.

Photocatalytsts	Band gap[a] (eV)	BET[b] (m^2 g^{-1})	Rate of H_2-production ($\mu mol\ h^{-1}$/ 5 mg)	Rate of H_2-production / BET surface area ($\mu mol\ h^{-1}\ m^{-2}$)	QY (%)
CdS NPs	2.36	16.25	0.85 ± 0.3	10.46	0.067±0.04
CdS MDs	2.32	4.80	Trace	Trace	Trace
3DHU-CdS	2.42	43.48	16.3 ± 0.5	74.98	0.76±0.06

[a] the band gap values were estimated from the UV-vis diffuse reflectance spectra;

[b] the surface area was calculated using the Brunauer-Emmett-Teller method.

Table S4. Summary of the band gap values and H_2 production rate of the 3DHU-CdS prepared at different temperatures.

Temperature (℃)	Band gap[a] (eV)	Rate of H_2-production (μmol h^{-1}/ 5 mg)	QY (%)
80	2.43	17.6 ± 0.6	0.83 ± 0.08
120	2.42	16.3 ± 0.5	0.76 ± 0.06
160	2.42	15.7 ± 0.4	0.72 ± 0.05
180	2.34	10.6 ± 0.7	0.41 ± 0.08
200	2.33	5.2 ± 0.3	0.20 ± 0.04
220	2.32	4.9 ± 0.3	0.19 ±0.04

[a] the band gap values were estimated from the UV-vis diffuse reflectance spectra.

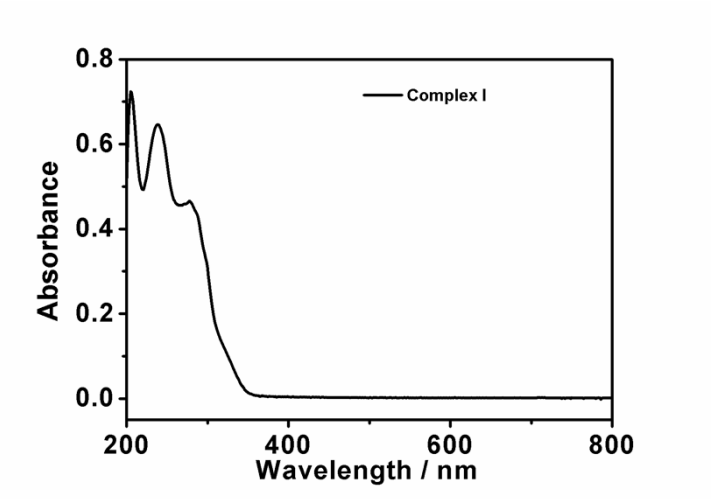

Fig. S15 UV-Vis absorption spectrum of Complex **I** in water.

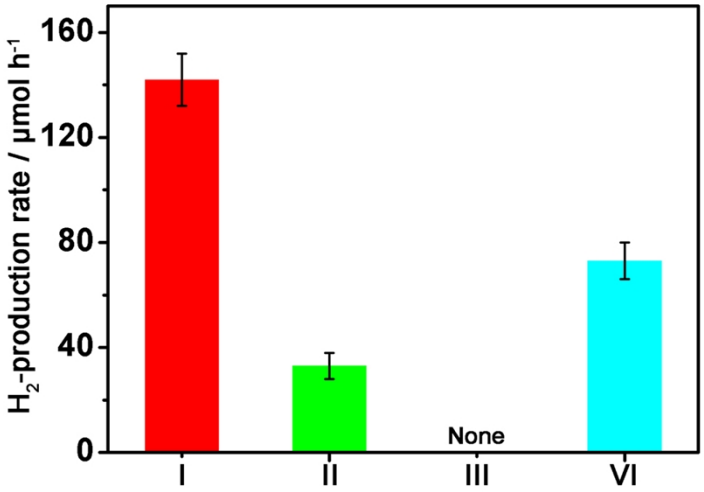

Fig. S16 H_2-production rate under different photocatalytic system containing 3DHU-CdS (5mg), Complex **I** (0.5mg) in (I) EtOH/H_2O (*V*:*V*=1:1) and 2 mL TEA, (II) EtOH/H_2O (*V*:*V*=1:1) without TEA, (III) EtOH and 2mL TEA, (VI) EtOH/H_2O (*V*:*V* =1:1) and 2 mL TEOA (triethanolamine). In this Figure, we can know that the H_2-production rate decreas sharply in the absence of TEA. On the other hand, when using the TEOA instead of TEA as the sacrificial agent, the rate experiences a decline. TEA as an efficient electron donor has been reported in the some literatures (Z. J. Han, WR. Mcnamara, M. S. Eum, P. L. Holland, R. Eisenberg, *Angew. Chem. Int. Ed.* 2012, 51, 1667-1670; Y. Xu, X. G. Yin, Y. Huang, P. W. Du, B. Zhang, *Chem. Eur. J.* 2015, 21, 4571-4575.). In addition, when photocatalytic system only contained EtOH and TEA, the H_2-production rate is none. This preliminary result suggests that the H_2 comes from the water reduction. In addition, our other control experiments (now shown here) reveal that the optimized conditions for the hybrid system of 3DHU-CdS and Complex **I** are 3DHU-CdS (5 mg), Complex **I** (0.5 mg), TEA (2 mL) in EtOH/H_2O (*V*:*V*=1:1).

Table S5. Summary of H_2 production rate of different CdS-based photocatalysts combing with Complex **I** (0.5 mg/30mL).

Photocatalysts	Rate of H_2-production ($\mu mol\ h^{-1}$)	QY (%)
CdS NPs	15.4 ± 3.1	0.6 ± 0.1
CdS MDs	10.0 ± 4.0	0.42 ±0.2
3DHU-CdS	145.1 ± 10.4	6.05 ±0.5

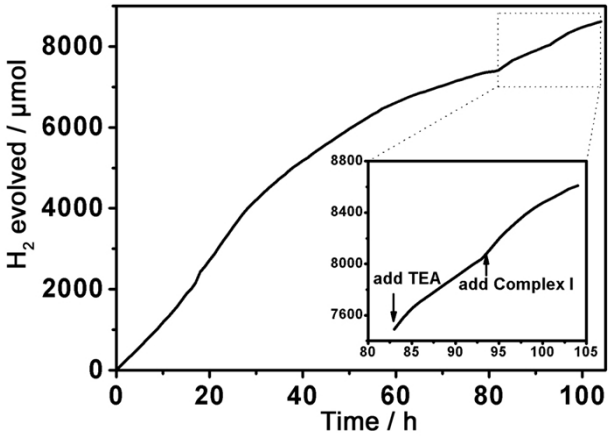

Fig. S17 Time course of hydrogen production from system containing 3DHU-CdS (5 mg), Complex **I** (0.5 mg), TEA (2 mL) in EtOH/H_2O (*V*:*V*=1:1) under visible light irradiation. The dates are the average values obtained from three independent experiments. After over 82 h irradiation, the re-addition of TEA and Ni complex successively restarted H_2 production. These results indicated that the deactivation of the system is mainly due to the decomposition of the Complex **I** and the TEA, and suggesting that the 3DHU-CdS is still active.

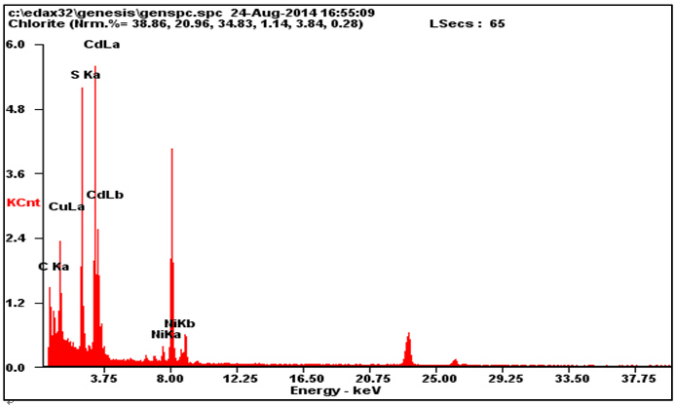

Element	Wt %	At %	K-Ratio	Z	A	F
C K	57.72	87.77	0.1528	1.0361	0.2554	1.0002
CuL	24.03	6.91	0.1019	0.9367	0.4523	1.0008
S K	5.77	3.29	0.0237	1.0160	0.3997	1.0113
CdL	12.42	2.02	0.1189	0.9069	1.0555	1.0000
NiK	0.07	0.02	0.0006	0.9781	0.8773	1.0000
Total	100.00	100.00				

Fig. S18 EDS spectra of 3DHU-CdS after 110 h photocatalytic test. Note that after irradiation, the amount of Ni present is negligible, suggesting that the Complex **I** do not be reduced to Ni(0) during the photocatalytic test.